Biointerface Research in Applied Chemistry
Open-Access Journal (ISSN: 2069-5837)

Article
Volume 13, Issue 3, 2023, 254
https://doi.org/10.33263/BRIAC133.254

BNB-BnNn Nano-Motor in Binding with ACC (tRNA) Nucleotides as an Amino Acid Detector in Ribosome: QM/MM & Monte Carlo Studies

Majid Monajjemi [1,*], Fatemeh Mollaamin [2]

[1] Department of chemical engineering, Central Tehran Branch, Islamic Azad University, Tehran, Iran
[2] Department of Biomedical Engineering, Faculty of Engineering and Architecture, Kastamonu University, Kastamonu, Turkey
* Correspondence: m_monajjemi@srbiau.ac.ir (M.M.); maj.monajjemi@iauctb.ac.ir (M.M.);
Scopus Author ID 6701810683

Received: 22.03.2022; Accepted: 20.04.2022; Published: 10.06.2022

Abstract: The electromagnetic non-bonded interactions of BNB molecule inside the B_nN_n (such as $B_{12}N_{12}$, $B_{15}N_{15}$, and $B_{18}N_{18}$) ring as a detector for tRNA-Amino acid conjugation has been investigated by QM/MM & Monte Carlo methods. In this study, we have shown that the BNB-B_nN_n systems can work as a nano rotor-stator for detecting tRNA during the tRNA-Amino-acid conjugation. We have employed the $B_{12}N_{12}$-tRNA (glu), $B_{12}N_{12}$–tRNA(phe) and $B_{12}N_{12}$-BNB-tRNA(arg) systems coupled with BN (-, 0, +) B inside the $B_{12}N_{12}$ ring (as a rotor) (n=12, 15, 18). We have shown that the tRNA as an extrinsic factor (stator) is set in the BNB- $B_{12}N_{12}$ system due to the generation of radical, anion, and cation forms of BN(-,0,+)B. We have also calculated the tRNA-BNB-$B_{12}N_{12}$ and obtained quantized transitional frequencies among the forms of radical, anionic, and cationic. The three frequencies have been yielded as νr-c) 486948.498 GHz, νa-c) 1792900.812 GHz, and νr-a) 2507076.816 GHz. It can be seen that all observed frequencies appeared in the IR and macro wave regions.

Keywords: tRNA; BnNn ring; ribosome; Monte Carlo.

1. Introduction

Genetic code translation relies on the correct aminoacylation of tRNAs by their cognate amino acyl-tRNA synthetase (aaRS) that catalyzes the formation of “charged” transfer RNA. Recognition is an essential part of this specific process, a function of different situations, including the tertiary structure of tRNA and its folding. aaRS must recognize and charge only cognate tRNA’s; therefore, they have to be able to distinguish cognate from non-cognate tRNA’s. Although aaRS binds to a particular amino acid and a molecule of ATP at its active site at the beginning of the process, the most important step is when a specific tRNA binds to the synthetase [1-3]. Except for some special mitochondrial transfer RNAs, every tRNA molecule consists of three loops and four stems. According to the size of the variable loop, tRNAs have divided into two classifications (Class I and II), while a large variable loop (between 13 and 21nucleotides) are class II and those groups with an extra short loop (four or five nucleotides) are class I [4,5]. $tRNA^{Ser}$ and $tRNA^{Leu}$ are generally placed into of class II group, while *E. coli* tRNATyr belongs to class II. In addition, yeast tRNATyr, is located in class I [6-8]. Synthetases can also be divided into classes based on their active site built near the ATP binding domain. The synthetase protein was characterized by its large structural

diversity [9-11]. The complexes between tRNA and aminoacyl-tRNA synthetases can be defined in two systems 1- a glutaminyl system for class I and a 2-aspartic system for class II. In the first one, the synthetase approaches the tRNA from the minor groove side, while the second one approaches the acceptor end stem from the major groove side [12]. In this work, we have concentrated on the tertiary structure of tRNA to investigate the mechanism of tRNA recognition and to bind to the synthetase for two classes. Although the tRNA sequences in the anticodon region, as well as other parts such as the acceptor stem, are important for the recognition, we have realized that the common ACC nucleotides (74-76) in all tRNAs have to save specific electromagnetic information that corresponds to the cognate synthetase in its structures. In our previous works [13-16], we have shown that the B_nN_n–BNB systems can work as a nano rotor-stator molecular motor for biological systems. The study for the B_nN_n-$BN^{(-,0,+)}$ B systems and then for Adenine-Thymine and Guanine-Cytosine base pairs coupled with $BN^{(-,0,+)}$ B inside the B_nN_n (n=8, 10, 12, 15, 18, 20, 24) have been investigated [15,16]. The ACC nucleotides from two classes of tRNAs coupled with $BN^{(-,0,+)}$ B inside the $B_{12}N_{12}$ ring for understanding the situation of electromagnetic potential and properties inside of ACC (Figure 1).

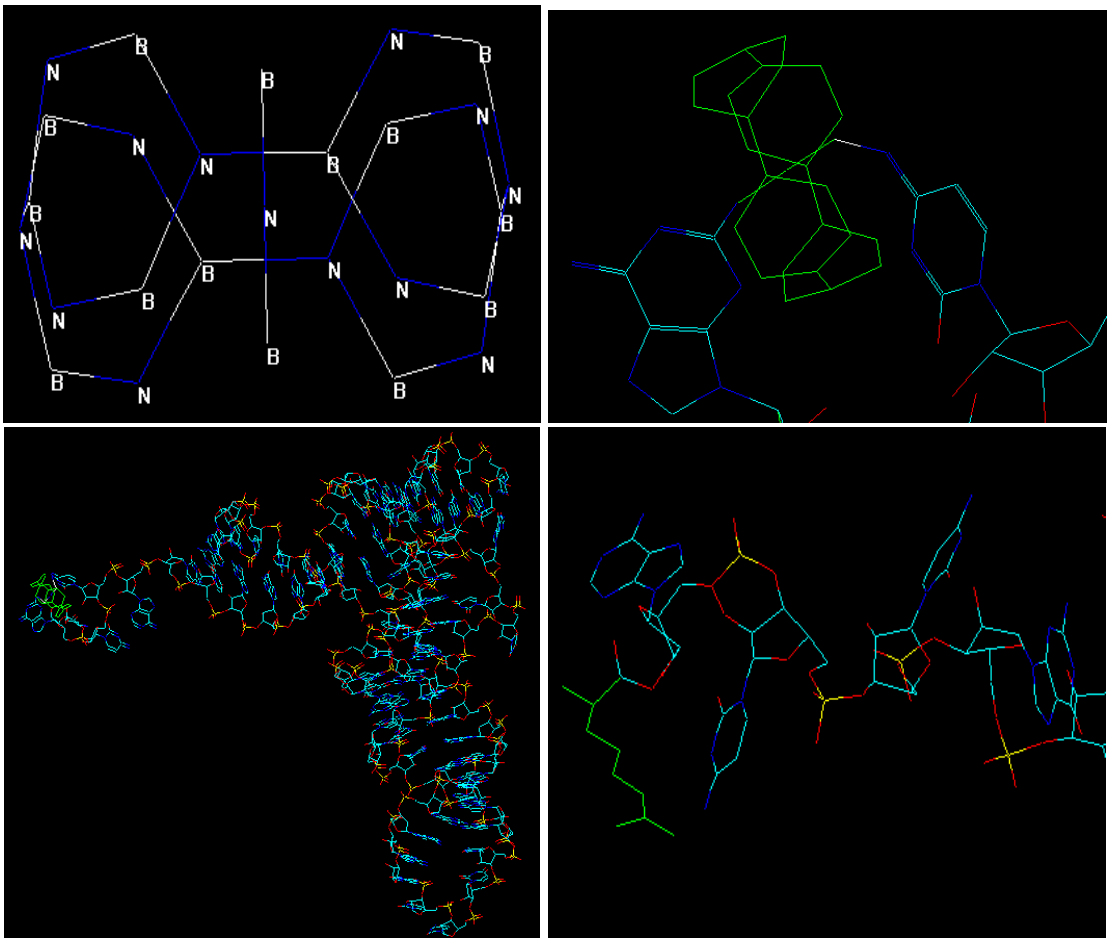

Figure 1. The ACC nucleotides from two classes of tRNAs coupled with $BN^{(-,0,+)}$ B inside the $B_{12}N_{12}$.

The four different structures of tRNAs, including $tRNA^{Phe}$, $tRNA^{Asp}$, $tRNA^{fMet}$, and *E. coli* $tRNA^{fMet}$ are known to have atomic resolution [17-21]. Yeast $tRNA^{Phe}$ and $tRNA^{Asp}$ were analyzed in two different shapes [17,19]. This concept was first demonstrated by the genetic experiments of Normanly and co-workers [22,23], who transferred the identity determinants of $tRNA^{Ser}$ into $tRNA^{Leu}$. A few noteworthy examples are those of $tRNA^{Ala}$ [24,25], with its

unique or at least major identity determinant (the third base pair of the acceptor stem G3:U70), $tRNA^{Gln,}$ and $tRNA^{ASP}$ [26]. Figure 2 presents the major identity nucleotide of yeast $tRNA^{Phe}$ and *E. coli* $tRNA^{Glu}$ and $tRNA^{Arg}$.

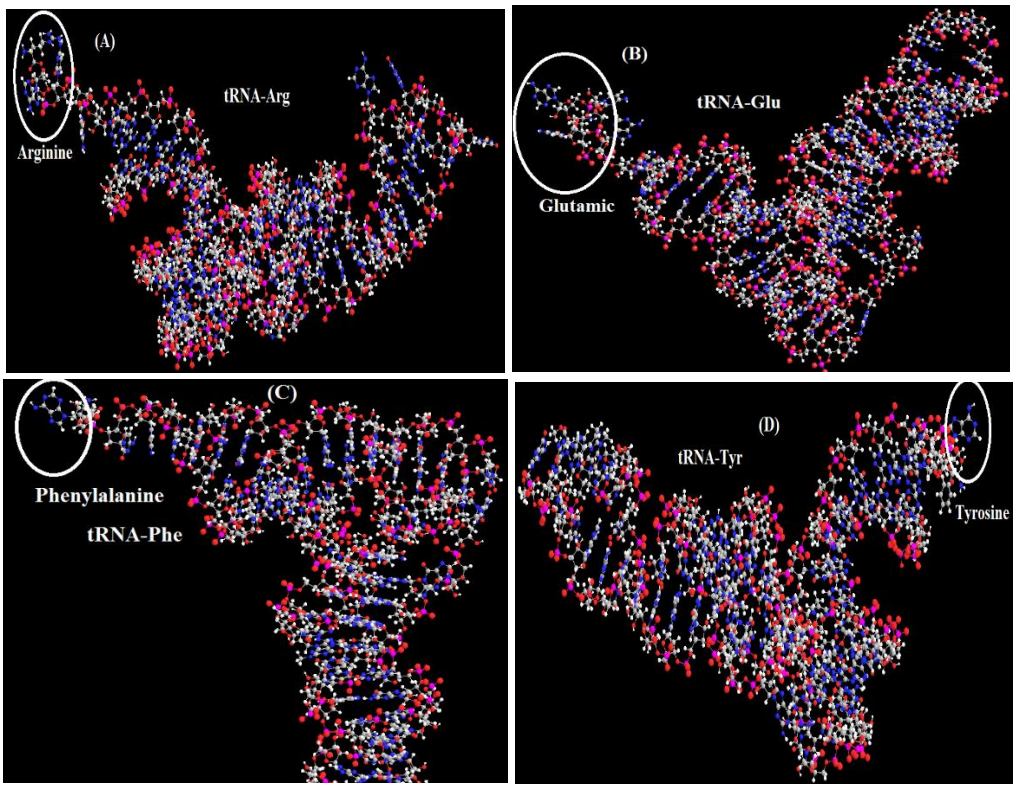

Figure 2. The major identity nucleotide of yeast $tRNA^{Phe}$ and *E. coli* $tRNA^{Glu}$, $tRNA^{Arg}$, and $tRNA^{Tyr}$.

2. Materials and Methods

2.1. The interactions between BNB-$B_{12}N_{12}$ and Tyrosine.

Figure 3 exhibits the structure of Tyrosine and BNB-$B_{12}N_{12}$ molecules at distance R. Particles $i \in$ Tyr and $j \in B_{12}N_{12}$ *Ring* are assumed in our model. The total Hamiltonian $H = H^{(0)} + H^{(1)}$ consists of two parts: (A) Free molecule of $H^{(0)} = H^{B12N12} + H^{Tyr}$ and (B) interaction operator of $H^{(1)} = \sum_{i \in Tyr} \sum_{j \in B_{12}N_{12}} \frac{q_i q_j}{r_{ij}}$. The loops and B-N bonds of $B_{12}N_{12}$ ring provide an external potential."$V_{(r_i)}$" for Tyr, which is $V_{(r_i)} = \sum_{j \in B12N12} \frac{q_j}{r_{ij}}$, thus, we have:$H^{(1)} = \sum_{i=1}^{n} q_i V(r_i) = \sum_{i=1}^{n} q_i V(x_i, y_i, z_i)$.

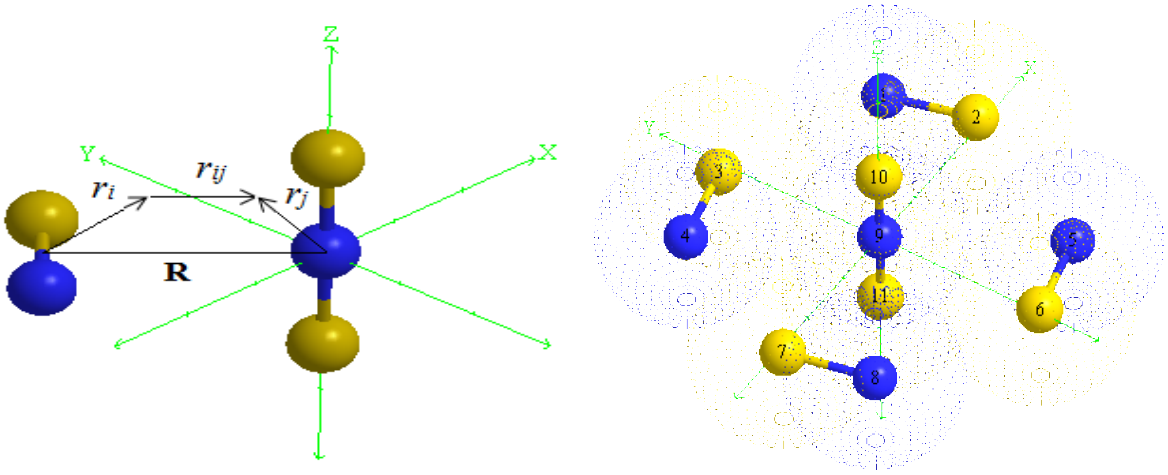

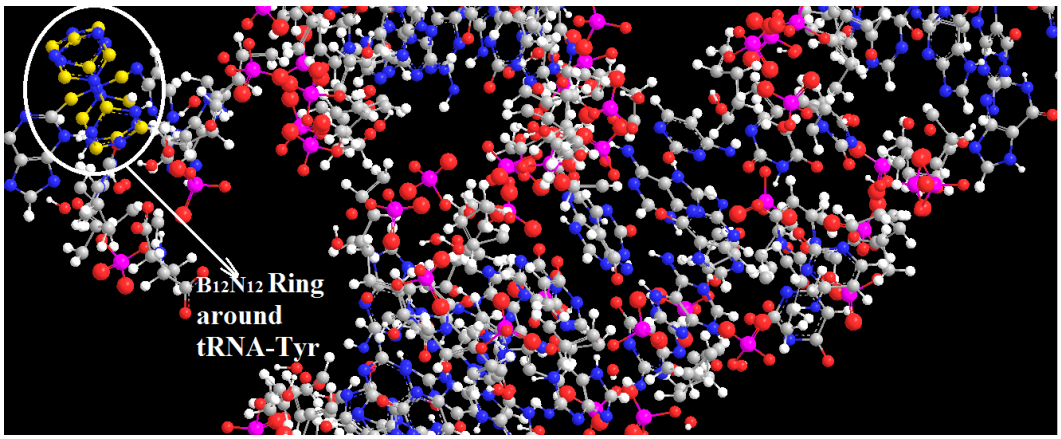

Figure 3. The Tyr and BNB-$B_{12}N_{12}$ ring structures at distance R : $i \in$ Tyr and $j \in B_{12}N_{12}$, ($r_i = (x_i, y_i, z_i)$ and $r_j = (x_j, y_j, z_j)$, R= (0, 0, R), r_{ij}=r_j-r_i+R.

Substitution into the $H^{(1)}$ after some rearrangements results in equation 1:

$$H^{(1)} = \frac{\sum_{(i=1)\in Tyr}^{n} \boldsymbol{q_i} \sum_{(j=1)\in B_{12}N_{12}}^{n} \boldsymbol{q_j}}{R} + \frac{\sum_{(i\in Tyr)}^{n} \boldsymbol{q_i r_i} q^{B_{12}N_{12}}}{R^2} - \frac{\sum_{(j\in Tyr)}^{n} \boldsymbol{q_j r_j} q^{BNB}}{R^2} + \frac{\mu_x^{BNB}\mu_x^{B_{12}N_{12}} + \mu_y^{BNB}\mu_y^{B_{12}N_{12}} - 2\mu_z^{Tyr}\mu_z^{B_{12}N_{12}}}{R^3} \quad (1)$$

Where the total charges are equal to $q^{Tyr} = \sum_{(i=1)\in BNB}^{n} q_i$, $q^{B_{12}N_{12}} = \sum_{(j=1)\in B_{12}N_{12}}^{n} q_j$ (and the dipole operators are $\mu^{TYr} = \sum_{(i=1)\in BNB}^{n} q_i\, r_i$, $\mu^{B_{12}N_{12}} = \sum_{(j=1)\in B_{12}N_{12}}^{n} q_j\, r_j$.

The interaction tensor's operator can be used as an alternative form of the dipole-dipole interaction operator as follows:

$$\frac{\mu_x^{TYr}\mu_x^{B_{12}N_{12}} + \mu_y^{TYr}\mu_y^{B_{12}N_{12}} - 2\mu_z^{Tyr}\mu_z^{BB_{12}N_{12}}}{R^3} = \frac{\mu^{TYr}\mu^{B_{12}N_{12}} - 3\mu_z^{TYr}\mu_z^{B_{12}N_{12}}}{R^3} = \frac{\mu^{Tyr}.\hat{\boldsymbol{T}}.\mu^{B_{12}N_{12}}}{R^3} \quad (2)$$

With the interaction tensor $\hat{T} = \begin{bmatrix} T_{xx} & T_{yy} & T_{zz} \\ T_{yx} & T_{yy} & T_{yz} \\ T_{zx} & T_{zy} & T_{zz} \end{bmatrix} = \begin{bmatrix} 1 & 0 & 0 \\ 0 & 1 & 0 \\ 0 & 0 & -2 \end{bmatrix}$.

Schrödinger equations of Tyr and $B_{12}N_{12}$ are: $H^{Tyr}\Phi_{K_1}^{Tyr} = E_{K_1}^{Tyr}\Phi_{K_1}^{Tyr}$ and $H^{\mathrm{B12N12}}\Phi_{K_1}^{\mathrm{B12N12}} = E_{K_1}^{\mathrm{B12N12}}\Phi_{K_1}^{\mathrm{B12N12}}$ and the eigenvalues of unperturbed terms ($H^{(0)}\Phi_K^{(0)} = E_K^{(0)}\Phi_K^{(0)}$ with $\Phi_K^{(0)} = \Phi_{K_1}^{Tyr}\Phi_{K_2}^{\mathrm{B12N12}}$) are $E_K^{(0)} = E_{K_1}^{A} + E_{K_2}^{B}$.

Therefore, the first-order energy can be indicated as in equation 10:

$$E_0^{(1)} = \langle \Phi_0^{(0)} | H^{(1)} | \Phi_0^{(0)} \rangle = \langle \Phi_0^{Tyr}\Phi_0^{BNB-\mathrm{B12N12}} | H^{(1)} | \Phi_0^{Tyr}\Phi_0^{\mathrm{BNB-B12N12}} \rangle \quad (3)$$

Including the multipole expansion of $H^{(1)}$, from which integration can be separated over the coordinates (x_i, y_i, z_i) and (x_j, y_j, z_j) of the particles $i \in$ Tyr and $j \in$ BNB-$B_{12}N_{12}$, while the permanent multipole moments are $< \mu^{Tyr} > = \langle \Phi_0^{Tyr} | \mu^{Tyr} | \Phi_0^{Tyr} \rangle$ and $< \mu^{\mathrm{B12N12}} > = \langle \Phi_0^{\mathrm{B12N12}} | \mu^{\mathrm{B12N12}} | \Phi_0^{\mathrm{B12N12}} \rangle$. The second-order energy is:

$$E_0^{(2)} = \sum_{k\neq 0} \frac{\langle \Phi_0^{(0)} | H^{(1)} | \Phi_K^{(0)} \rangle \langle \Phi_K^{(0)} | H^{(1)} | \Phi_0^{(0)} \rangle}{E_0^{(0)} - E_k^{(0)}} \quad (4)$$

Where the index k that labels the excited states of the system is a composite index: k = (k_1, K_2), the summation over k≠ 0 can be split into three sums, with $k_1 \neq 0$ and $K_2 = 0$ for Tyr excited molecule, $k_2 \neq 0$ and $k_1 = 0$ for $B_{12}N_{12}$ excited molecule, and k_1, $k_2 \neq 0$ for both excited molecules. The Tyr can be exited to higher energy levels with the $B_{12}N_{12}$ ring surrounding it, which can form the basis for more detailed studies of other non-bonded interacting systems. The electrostatic interactions of the Tyr with four loops of the $B_{12}N_{12}$ ring within the vertical transition, the three loops have been frozen, and the electrostatic interaction of Tyr with the

one remaining active loop has been taken into account. Based on previous studies [27-82], dipole expansions are used to study electromagnetic fields of charge and current distributions. It is only for the clustered system with large density fluctuation that such a fast method has superior efficiency.

2.2. Computational details.

2.2.1.abinitio calculation

The EPR-II basis sets are used for B to, and EPR-III is improved to describe the nuclear region for B to F. The active space for the CASSCF method was employed and, 11 active electrons and 12 active orbitals were considered for $B_2N^{(0)}$ and 10 and 12 electrons for $B_2N^{(+)}$and $B_2N^{(-)}$, respectively. The BNB has been optimized by CASSCF (11, 12)/cc-pvqz and CASSCF (11, 12)/AUG-cc-pvqz (for radical) and CASSCF (10, 12)/cc-pvqz for cation. Polarizabilities and hyperpolarizabilities have been computed by CISD and QCISD, and CASSCF methods and double numerical differentiation of energies have been used by pol=En only keyword in some cases.

2.2.2 MD simulations and docking.

We accomplished three categories of MD simulations: (1) blank system, (2) Isolated BnNn ring, and (C) tRNA nucleosides in B12N12-BNB-tRNA. While the simulation setups are not equal for the three categories, the methodology and run parameters were the same. The simulation box dimension was 5.0× 10.0 × 15.0 nm3 for all simulations. For the Isolated BnNn ring simulations (B and N), Visual Molecular Dynamics (VMD 1.9.2 version) software was used to generate a ring BnNn model with B–N bond length of 1.4 Angstrom and ring dimensions of r= 5.0 nm. A simulation box of the above-mentioned dimensions was created with a radius with a BNB at the center. The nucleoside is placed at the center of the ring before the addition of water molecules. We used force-field parameters from amber employing Chen-Garcia corrections for nucleoside-BNB-$B_{12}N_{12}$ interactions. The LJ parameters have been evaluated carefully and were parameterized against contact angles of water on the B_nN_n center.

BIOVIA_2020 software has been used for docking, and the grids between 20-25 Å were done over the co-crystallized aging and Parkinson mutation genome. Re-docking of the molecules was done to consider docking protocols. The docked shapes were evaluated based on crystal structures of related proteins for calculating the root mean square deviation. The re-docking of macromolecules poses with 1.20Å RMSD. Lower RMSD indicates the methodologies are adequate and could be used to search for any further inhibitors. Docking was done in 3 different modes, virtual screening followed by standard-precision (SP) and extra-precision (XP) docking using the Glide program. In this research, the iGEMDOCK has been used, and the acceptable receptor can be defined for the binding site in whole protein structures. iGEMDOCK can help quickly define the suitable binding site based on energy Gibbs amounts and docking simulation steps as follows: (1), Prepare Binding Site on the Protein-Ligand. (2) Browsing and selecting the protein file. (3) Defining the binding site type as a bounded ligand. (4) Defining the center of the binding site by selected ligand. (5) Setting the size of the binding site through the extended radius from the selected ligand. IGEMDOCK yields analysis information that can be visualized as the docked states and items via protein-ligand interactions. Consequently, the prediction and scores of ligands can be saved in the output

routs. The optimum energy poses of each system will be outputted into the location of "best: Pose". Via looking at the bounded structures of several ligands, they can be selected by the check box of the ligand. If the co-crystallized ligands are retained on the binding site structures, it will be predicted poses. Cluster analysis is the partitioning of a data set into subsets. These are based on interaction and atomic combination aspects. Interaction aspects are extracted from the macromolecule couples, and atomic structures are calculated via atomic types.

2.3. tRNA processing and modification.

The complete data were obtained with the phosphate alkylating reagent ethylnitrosourea [83-92]. The conformational changes are not sequence-specific; for example, the acceptor stem ends of *E. coli* tRNA and yeast tRNA-ASP are identical, but their complex state is quite different [93-100]. The first step toward that generalization within class I synthetizes was made with the modeling of the complex between MetRS and its cognate tRNA [101-105]. Usually, they can only be charged by their cognate mitochondrial synthetases[106-108]. The crystal structure of four different tRNAs (yeast tRNA', tRNAASP, tRNAet, and *E. coli* tRNAt) are known to have the atomic resolution. Yeast tRNAHe and tRNAASP were analyzed in two crystal forms [106-110].

3. Results and Discussion

Produce of hydrogen bonds to amino protons in nucleic acids is accompanied by downfield shifts in the NMR signals of the protons and nitrogen in the amino units. Interactions that shift the protons and nitrogen to the lower field can be modeled with appropriately substituted nucleosides in chloroform. Model studies of hydrogen bond donors and acceptors have been very helpful for assigning IH15N resonances of related interactions in nucleic acids. Proton chemical shifts for monomeric U and s4U and UA and s4UA base pairs are well characterized in nucleoside models (Figure 4).

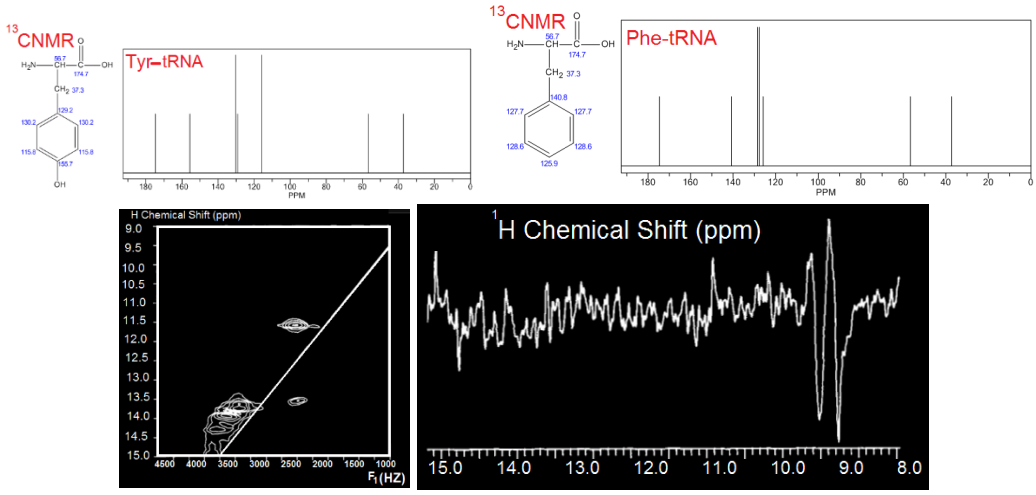

Figure 4. NMR position of aminoacids-tRNA.

In this region, native tRNAThr contains three modified nucleosides, 3-methylcytidine (m3C32), inosine (134), and N-((9-3-D-ribofuranosylpurine-6-yl)carbamoyl)threonine (t6A37) . The first position of the anticodon seems unlikely to be involved in the base-specific recognition by ThrRS since tRNAThr isoacceptors belonging to a four-codon box have at least two kinds of bases at this position (figure 5). Several factors were considered in using the biochemical data to conclude the mechanisms by which SerRS recognizes these base pairs.

Based on previous tRNASer footprinting and X-ray crystallographic studies of the tRNASer-SerRS complex, it was clear that SerRS primarily binds from the variable loop side of the tRNA. This orients SerRS toward the major rather than the minor groove of the acceptor stem helix. Although each base pair presents a distinctive array of major groove hydrogen bond donors, acceptors, and hydrophobic groups, their accessibility to amino acid side chains is predicted to be greater at positions 1-72 and 2-71 than at positions 4-69 and 5-68 due to differences in the proximity of each base pair to the helix.

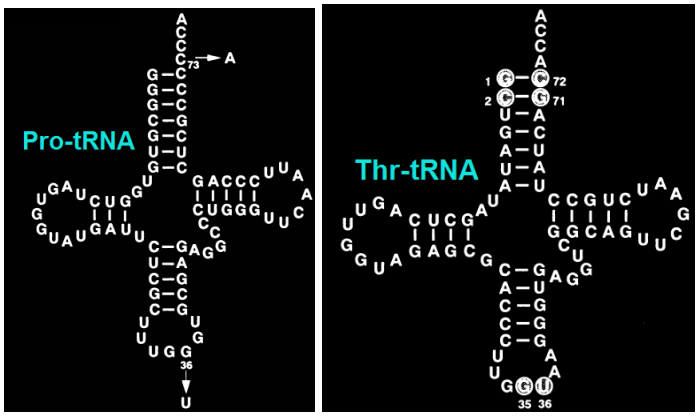

Figure 5. The yeast Pro-tRNAPrO and Thr-tRNA transcript for the aminoacylation specificity conversion.

Site-directed mutagen has been the main tool for protein engineering, and it permits various amino acids in proteins to be substituted by any of the other 20 natural amino acids. But the chemical invariance of the 20 natural amino acids limits our ability to manipulate the structure and function of proteins. In the recent decade, attempts have been made to expand the set of amino acids as building blocks for biomacromolecules. One important approach is using chemically misacylated tRNA as the non-natural amino acid supplier and nonsense codon or stopping codon as the sense codon for this non-coded amino acid to site-specifically insert this amino acid to the programmed site of proteins. Approximately, the non-natural amino acid of interest is chemically linked to the suppressor tRNA, consisting of an anticodon corresponding to the UAG codon. This chemically charged tRNA is added to a cell system, the suppressor tRNA decodes the related codon, and the non-natural amino acid is inserted in the intended site of the protein. One of the major points of this method is choosing the appropriate suppressor tRNA; the charged suppressor tRNA should not be acylated or deacylated by any of the aminoacyl-tRNA Synthetizes presented in the translation system. By co-injection of charged suppressor tRNA and amber-encoded mRNA into Xenopus oocytes, they introduced non-natural amino acids into the α-subunit of the nicotinic acetylcholine receptor. Moreover, four codon suppression, use of an unassigned codon, and non-natural base paring have been exploited in this chemically misacylated tRNA method to incorporate non-natural amino acids to improve translation efficiency and achieve the possibility of introducing multiple non-protein. In addition, the early success of site-specific incorporation of novel amino acids in vivo in *E. coli* can expression system. One of the most critical requirements for this method to work is orthogonality; to prevent the misincorporation of natural amino acids into the amber site and misincorporation of the 21st amino acid into sites other than the intended amber site, the introduced aaRS can only recognize the non-natural amino acid and catalyze the attachment of this amino acid exclusively.

4. Conclusions

tRNA-recognition by the BNB-BnNn ring detector exhibits two distinct features. The electromagnetic non-bonded interactions of BNB molecule inside the B_nN_n (such as $B_{12}N_{12}$, $B_{15}N_{15}$, and $B_{18}N_{18}$) ring as a detector for tRNA-Amino acid conjugation has been investigated by QM/MM & Monte Carlo methods. In this study, we have shown that the BNB-B_nN_n systems can work as a nano rotor-stator for detecting tRNA during the tRNA-Amino-acid conjugation. The complexes between tRNA and aminoacyl-tRNA synthetases can be defined in two systems 1- glutaminyl system for class I and a 2-aspartic system for class II. In the first one, the synthetase approaches the tRNA from the minor groove side, while the second one approaches the acceptor end stem from the major groove side. Two structural solutions, one for each class of synthesizes, can then be predicted. This general model of interaction does not exclude the specificity of recognition. These interactions involve different protein modules attached to the NH2- or COOH-terminal ends of the active site domain or inserted at constant positions of the ATP binding folds.

Funding

This research received no external funding.

Acknowledgments

The authors thanks Kastamonu University and Islamic Azad University for providing computer and software equipments.

Conflicts of Interest

The authors declare no conflict of interest.

References

1. Schimmel, P. Aminoacyl-tRNA synthetases: general scheme of structure-function relationships in the polypeptides and recognition of transfer RNAs. *Annu. Rev. Biochem.* **1987**, *56*, 125-158, https://doi.org/10.1146/annurev.bi.56.070187.001013.
2. Lapointe, J. Mechanism and evolution of multidomain aminoacyl-tRNA synthetases revealed by their inhibition by analogues of a reaction intermediate, and by properties of truncated forms.*Journal of Biomedical Science and Engineering* **2013**, *6*, 943-946, https://doi.org/10.4236/jbise.2013.610115.
3. Soll, D. The accuracy of aminoacylation - ensuring the fidelity of the genetic code. Experientia **1990**, *46*, 1089-1096, https://doi.org/10.1007/BF01936918.
4. Kim, S.H.; Suddath, F.L.; Quigley, G.J.; McPherson, A.; Sussman, J.L.; Wang, A.H.J.; Seeman, N.C.; Rich, A. Three dimensional tertiary structure of yeast phenylalanine transfer RNA. *Science* **1974**, *185*, 435-440, https://doi.org/10.1126/science.185.4149.435.
5. Robertus, J. D.; Ladner, J. E.; Finch, J.T. Rhodes, D; Brown, R.S.; Clark, B.F.C.; KIug, A. Structure of yeast phenylalanine tRNA at 3 A resolution. *Nature (London)* **1974**, *250*, 546-551, https://doi.org/10.1038/250546a0.
6. Stout, C.D.; Mizuno, H.; Rubin, J.; Brennan, T.; Rao, S.T.; Sundaralingam, M. Atomic coordinates and molecular conformation of yeast phenylalanyl tRNA. An independent investigation. *Nucleic Acids Res.* **1976**, *4*, 1111–1123, https://doi.org/10.1093/nar/3.4.1111.
7. Moras, D.; Comarmond, M.B.; Fischer, J.; Weiss, R.; Thierry, J. C.; Ebel, J.P.; Giegé, R. Crystal structure of yeast tRNAA. *Nature (London)* **1980**, *288*, 669-674, https://doi.org/10.1038/288669a0.
8. Woo, N.H.; Roe, B.A.; Rich, A.Three-dimensional structure of Escherlchia coli initiator $tRNA_f^{Met}$. *Nature (London)* **1980**, *286*, 346-351, https://doi.org/10.1038/286346a0.
9. Burbaum, J.; Starzyk, R.M.; Schimmel, P. Understanding structural relationships in proteins of unsolved three-dimensional structure. *Proteins* **1990**, *7*, 99-111, https://doi.org/10.1002/prot.340070202.
10. Tzagoloff, A.; Gatti, D.; Gampel, A. Mitochondnal aminoacyl-tRNA synthetases. *Prog. Nucleic Acid Res. Mol. Biol* **1990**, *39*, 129-158, https://doi.org/10.1016/S0079-6603(08)60625-X.

11. Mirande, M. Aminoacyl-tRNA synthetase family from prokaryotes and eukaryotes: structural domains and their implications. *Prog. Nucleic Acid Res. Mol. Biol* **1991**, *40*, 95-142, https://doi.org/10.1016/s0079-6603(08)60840-5.
12. Cavarelli , J.; Moras, D. Recognition of tRNAs by aminoacyl-tRNA synthetases. *The FASEB Journal* **1993**, 7, 79-86, https://doi.org/10.1096/fasebj.7.1.8422978.
13. Lee, V.S.; Nimmanpipug, P.; Mollaamin, F.; Thanasanvorakun, S.; Monajjemi, M. Investigation of single wall carbon nanotubes electrical properties and normal mode analysis: Dielectric effects. *Russian Journal of Physical Chemistry A* **2009**, *83*, 2288-2296, https://doi.org/10.1134/S0036024409130184.
14. Monajjemi, M.; Boggs, J.E. A New Generation of BnNn Rings as a Supplement to Boron Nitride Tubes and Cages. *J. Phys. Chem. A* **2013**, *117*, 1670-1684, http://dx.doi.org/10.1021/jp312073q.
15. Monajjemi, M. Quantum investigation of non-bonded interaction between the B15N15 ring and BH2NBH2 (radical, cation, and anion) systems: a nano molecularmotor. *Struct Chem* **2012,** *23*, 551–580, http://dx.doi.org/10.1007/s11224-011-9895-8.
16. Monajjemi, M. Non bonded interaction between BnNn (stator) and BN B (rotor) systems: A quantum rotation in IR region. *Chemical Physics* **2013**, *425*, 29-45, https://doi.org/10.1016 /j.chemphys.2013.07.014.
17. Kim,S.H.; Quigley, G.; Suddath, F.L.; McPherson, A.; Sneden, D.; Kim, J.J.; Weinzierl, J.; Blattmann, P.; Rich, A. The three-dimensional structure of yeast phenylalanine transfer RNA: shape of the molecule at 5.5-A resolution. *Proc Natl Acad Sci U SA.* **1972**, *69*, 3746-50, https://doi.org/10.1073/pnas.69.12.3746.
18. Suddath, F.L.; Quigley, G.J.; McPherson, A.; Sneden, D.; Kim, J.J.; Kim, S.H.; Rich, A. Three-dimensional structure of yeast phenylalanine transfer RNA at 3.0angstroms resolution. *Nature* **1974**, *248*, 20-4, https://doi.org/10.1038/248020a0.
19. Ruff, M.; Mitschler, A.; Cavarelli, J.; Giege, R.; Mikol, V.; Thierry, J.C.; Lorber, B.; Moras, D. A high resolution diffracting crystal form of the complex between yeast tRNAAsp and aspartyl-tRNA synthetase. *J. Mol. Biol.* **1988**, *201*, 235-236, https://doi.org/10.1016/0022-2836(88)90450-0.
20. Marcia, M.; Humphris-Narayanan, E.; Keating, K.S.; Somarowthu, S.; Rajashankar, K.; Pyle, A.M. Solving nucleic acid structures by molecular replacement: examples from group II intron studies. *Acta Cryst.* **2013**, *D69*, 2174-2185, https://doi.org/10.1107/S0907444913013218.
21. Aström, S.U.; von Pawel-Rammingen, U.; Byström, A.S. The yeast initiator tRNAMet can act as an elongator tRNA(Met) in vivo. *J Mol Biol*. **1993**, *233*, 43-58, https://doi.org/10.1006/jmbi.1993.1483.
22. Normanly, J.; Ogden, R.C.; Horvath, S.J.; and Abelson, J. Changing the identity of a transfer RNA .*Nature (London)* **1986**, *321*, 213-219, https://doi.org/10.1038/321213a0.
23. Normanly, J.; Ollick, T.; Abelson, J. Eight base changes are sufficient to convert a leucine-inserting tRNA into a serine-inserting tRNA. *Proc. Natl. Acad. Sci. U.S.A.* **1992**, *89*, 5680-5684, https://doi.org/10.1073/pnas.89.12.5680.
24. Hou, Y.M.; Schimmel, P. A simple structural feature is a major determinant of the identity of a transfer RNA. *Nature (London)* **1988**, *333*, 140-145, https://doi.org/10.1038/333140a0.
25. McCiain, W. H.; Foss, K. Changing the Identity of a tRNA by Introducing a G-U Wobble Pair Near the 3′ Acceptor End. *Science* **1988**, *240*, 793-796, https://doi.org/10.1126/science.2452483.
26. Putz, J.; Puglisi, J. D.; Florentz, C.; Giegé, R. Additive, cooperative and anti-cooperative effects between identity nucleotides of a tRNA. *Science* **1991**, *252*, 1696-1699, https://doi.org/10.1002/j.1460-2075.1993.tb05957.x.
27. Mollaamin, F.; Monajjemi, M. DFT outlook of solvent effect on function of nano bioorganic drugs. *Physics and Chemistry of Liquids* **2012**, *50*, 596-604, https://doi.org/10.1080/00319104.2011.646444.
28. Mollaamin, F.; Gharibe, S.; Monajjemi, M. Synthesis of various nano and micro ZnSe morphologies by using hydrothermal method. *Phys. Sci. Int. J.* **2011**, *6*, 1496-1500, https://doi.org/10.5897/IJPS10.260.
29. Monajjemi M. Graphene/(h-BN)*n*/X-doped raphene as anode material in lithium ion batteries (X = Li, Be, B AND N,). *Maced. J. Chem. Chem. Eng.* **2017**, *36*, 101–118, http://dx.doi.org/10.20450/mjcce.2017.1134.
30. Monajjemi, M. Cell membrane causes the lipid bilayers to behave as variable capacitors: A resonance with self-induction of helical proteins. *Biophysical Chemistry* **2015**, *207*, 114-127, https://doi.org/10.1016/j.bpc.2015.10.003.
31. Monajjemi, M. Study of CD5+ Ions and Deuterated Variants (CHxD(5-x)+): An Artefactual Rotation. *Russian Journal of Physical Chemistry A* **2018,** *92***,** 2215-2226, https://doi.org/10.1134/S0036024418110286.
32. Monajjemi, M. Liquid-phase exfoliation (LPE) of graphite towards graphene: An ab initio study. *Journal of Molecular Liquids* **2017**, *230*, 461–472, https://doi.org/10.1016/j.molliq.2017.01.044.
33. Jalilian, H.; Monajjemi, M. Capacitor simulation including of X-doped graphene (X = Li, Be, B) as twoelectrodes and (h-BN)m (m = 1–4) as the insulator. *Japanese Journal of Applied Physics* **2015**, *54*, 085101-7, https://doi.org/10.7567/JJAP.54.085101.
34. Ardalan, T.; Ardalan, P.; Monajjemi, M. Nano theoretical study of a C 16 cluster as a novel material for vitamin C carrier. *Fullerenes Nanotubes and Carbon Nanostructures* **2014**, *22*, 687-708, https://doi.org/10.1080/1536383X.2012.717561.
35. Mahdavian, L.; Monajjemi, M.; Mangkorntong, N. Sensor response to alcohol and chemical mechanism of carbon nanotube gas sensors *Fullerenes Nanotubes and Carbon Nanostructures* **2009**, *17*, 484-495, https://doi.org/10.1080/15363830903130044.

36. Monajjemi, M.; Najafpour, J. Charge density discrepancy between NBO and QTAIM in single-wall armchair carbon nanotubes. *Fullerenes Nanotubes and Carbon Nano structures* **2014**, *22*, 575-594, https://doi.org/10.1080/1536383X.2012.702161.
37. Monajjemi, M.; Hosseini, M.S. Non bonded interaction of B16 N16 nano ring with copper cations in point of crystal fields. *Journal of Computational and Theoretical Nanoscience* **2013**, *10*, 2473-2477, https://doi.org/10.1166/jctn.2013.3233.
38. Monajjemi, M.; Mahdavian, L.; Mollaamin, F. Characterization of nanocrystalline silicon germanium film and nanotube in adsorption gas by Monte Carlo and Langevin dynamic simulation. *Bulletin of the Chemical Society of Ethiopia* **2008**, *22*, 277-286, https://doi.org/10.4314/bcse.v22i2.61299.
39. Bakhshi, K.; Mollaamin, F.; Monajjemi, M. Exchange and Correlation Effect of Hydrogen Chemisorption on Nano V(100) Surface: A DFT Study by Generalized Gradient Approximation (GGA). *Journal of Computational and Theoretical Nanoscience* **2011**, *8*, 763-768, https://doi.org/10.1166/jctn.2011.1750.
40. Mollaamin, F.; Najafpour, J.; Ghadami, S.; Akrami, M.S.; Monajjemi, M. The electromagnetic feature of B N H (x = 0, 4, 8, 12, 16, and 20) nano rings:Quantum theory of atoms in molecules/NMR approach. *Journal of Computational and Theoretical Nanoscience* **2014**, *11*, 1290-1298. https://doi.org/10.1166/jctn.2014.3495.
41. Monajjemi, M.; Mahdavian, L.; Mollaamin, F.; Honarparvar, B. Thermodynamic investigation of enolketo tautomerism for alcohol sensors based on carbon nanotubes as chemical sensors. *Fullerenes Nanotubes and Carbon Nanostructures* **2010**, *18*, 45-55, https://doi.org/10.1080/15363830903291564.
42. Monajjemi, M.; Ghiasi, R.; Seyed, S.M.A. Metal-stabilized rare tautomers: N4 metalated cytosine (M = Li, Na, K, Rb and Cs), theoretical views. *Applied Organometallic Chemistry* **2003**, *17*, 635-640, https://doi.org/10.1002/aoc.469.
43. Ilkhani, A.R.; Monajjemi, M. The pseudo Jahn-Teller effect of puckering in pentatomic unsaturated rings C AE, A=N, P, As, E=H, F, Cl. *Computational and Theoretical Chemistry* **2015**, *1074*, 19-25, http://dx.doi.org/10.1016%2Fj.comptc.2015.10.006.
44. Monajjemi, M. Non-covalent attraction of B N and repulsion of B N in the B N ring: a quantum rotatory due to an external field. *Theoretical Chemistry Accounts* **2015**, *134*, 1-22.
45. Monajjemi, M.; Naderi, F.; Mollaamin, F.; Khaleghian, M. Drug design outlook by calculation of second virial coefficient as a nano study. *Journal of the Mexican Chemical Society* **2012**, *56*, 207-211, https://doi.org/10.29356/jmcs.v56i2.323.
46. Monajjemi, M.; Bagheri, S.; Moosavi, M.S. Symmetry breaking of B2N(-,0,+): An aspect of the electric potential and atomic charges. *Molecules* **2015**, *20*, 21636-21657, https://doi.org/10.3390/molecules201219769.
47. Monajjemi, M.; Mohammadian, N.T. S-NICS: An aromaticity criterion for nano molecules. *Journal of Computational and Theoretical Nanoscience* **2015**, *12*, 4895-4914, https://doi.org/10.1166/jctn.2015.4458.
48. Monajjemi, M.; Ketabi, S.; Hashemian, Z.M.; Amiri, A. Simulation of DNA bases in water: Comparison of the Monte Carlo algorithm with molecular mechanics force fields. *Biochemistry (Moscow)* **2006**, *71*, 1-8, https://doi.org/10.1134/s0006297906130013.
49. Monajjemi, M.; Lee, V.S.; Khaleghian, M.; Honarparvar, B.; Mollaamin, F. Theoretical Description of Electromagnetic Nonbonded Interactions of Radical, Cationic, and Anionic NH2BHNBHNH2 Inside of the B18N18 Nanoring. *J. Phys. Chem C* **2010**, *114*, 15315-15330, https://doi.org/10.1021/jp104274z.
50. Sarasia, E.M.; Afsharnezhad, S.; Honarparvar, B.; Mollaamin, F.; Monajjemi, M. Theoretical study of solvent effect on NMR shielding tensors of luciferin derivatives. *Phys Chem Liquids* **2011**, *49*, 561-571, https://doi.org/10.1080/00319101003698992.
51. Monajjemi, M.; Mollaamin, F.; Gholami, M.R.; Yoosbashizadeh, H.; Sadrnezhad, S.K.; Passdar, H. Quantum Chemical Parameters of Some Organic Corrosion Inhibitors, Pyridine, 2-Picoline 4-Picoline and 2, 4-Lutidine, Adsorption at Aluminum Surface in Hydrocholoric and Nitric Acids and Comparison Between Two Acidic Media. *Main Group Met. Chem.* **2003**, *26*, 349-362, https://doi.org/10.1515/MGMC.2003.26.6.349.
52. Monajjemi, M.; Robert, W.J.; Boggs, J.E. NMR contour maps as a new parameter of carboxyl's OH groups in amino acids recognition: A reason of tRNA–amino acid conjugation. *Chemical Physics* **2014**, *433*, 1-11, https://doi.org/10.1016/j.chemphys.2014.01.017.
53. Mollaamin, F.; Monajjemi, M.; Salemi, S.; Baei, M.T. A Dielectric Effect on Normal Mode Analysis and Symmetry of BNNT Nanotube. *Fuller. Nanotub. Carbon Nanostructures* **2011**, *19*, 182-196, https://doi.org/10.1080/15363831003782932.
54. Monajjemi, M. Metal-doped graphene layers composed with boron nitride–graphene as an insulator: a nanocapacitor. *Journal of Molecular Modeling* **2014**, *20*, https://doi.org/10.1007/s00894-014-2507-y.
55. Mollaamin, F.; Monajjemi, M.; Mehrzad, J. Molecular Modeling Investigation of an Anti-cancer Agent Joint to SWCNT Using Theoretical Methods. *Fullerenes, Nanotubes and Carbon Nanostructures* **2014**, *22*, 738-751, https://doi.org/10.1080/1536383X.2012.731582.
56. Monajjemi, M.; Ketabi, S.; Amiri, A. Monte Carlo simulation study of melittin: protein folding and temperature ependence. *Russian journal of physical chemistry* **2006**, *80*, S55-S62, https://doi.org/10.1134/S0036024406130103.

57. Monajjemi, M.; Heshmata, M.; Haeria, H.H. QM/MM model study on properties and structure of some antibiotics in gas phase: Comparison of energy and NMR chemical shift. *Biochemistry (Moscow)* **2006**, *71*, S113-S122, https://doi.org/10.1134/S0006297906130190.
58. Monajjemi, M.; Afsharnezhad, S.; Jaafari, M.R.; Abdolahi, T.; Nikosade, A.; Monajemi, H. NMR shielding and a thermodynamic study of the effect of environmental exposure to petrochemical solvent on DPPC, an important component of lung surfactant. *Russian Journal of Physical Chemistry A* **2007**, *81*, 1956-1963, https://doi.org/10.1134/S0036024407120096.
59. Mollaamin, F.; Noei, M.; Monajjemi, M.; Rasoolzadeh, R. Nano theoretical studies of fMET-tRNA structuren in protein synthesis of prokaryotes and its comparison with the structure of fALA-tRNA. *African journal of microbiology research* **2011**, *5*, 2667-2674, https://doi.org/10.5897/AJMR11.310.
60. Monajjemi, M.; Heshmat, M.; Haeri, H.H.; Kaveh, F. Theoretical study of vitamin properties from combined QM-MM methods: Comparison of chemical shifts and energy. *Russian Journal of Physical Chemistry* **2006**, *80*, 1061-1068, https://doi.org/10.1134/S0036024406070119.
61. Monajjemi, M.; Chahkandi, B. Theoretical investigation of hydrogen bonding in Watson–Crick, Hoogestein and their reversed and other models: comparison and analysis for configurations of adenine–thymine base pairs in 9 models. *Journal of Molecular Structure: THEOCHEM* **2005**, *714*, 43-60, https://doi.org/10.1016/j.theochem.2004.09.048.
62. Monajjemi, M.; Honarparvar, B.; Haeri, H.H.; Heshmat, M. An ab initio quantum chemical investigation of solvent-induced effect on 14N-NQR parameters of alanine, glycine, valine, and serine using a polarizable continuum model. *Russian Journal of Physical Chemistry* **2006**, *80*, S40-S44, https://doi.org/10.1134/S0036024406130073.
63. Monajjemi, M.; Seyed Hosseini, M. Non Bonded Interaction of B16N16 Nano Ring with Copper Cations in Point of Crystal Fields. *Journal of Computational and Theoretical Nanoscience* **2013**, *10*, 2473-2477, https://doi.org/10.1166/jctn.2013.3233.
64. Monajjemi, M.; Farahani, N.; Mollaamin, F. Thermodynamic study of solvent effects on nanostructures: phosphatidylserine and phosphatidylinositol membranes. *Physics and Chemistry of Liquids* **2012**, *50*, 161-172, https://doi.org/10.1080/00319104.2010.527842.
65. Monajjemi, M.; Ahmadianarog, M. Carbon Nanotube as a Deliver for Sulforaphane in Broccoli Vegetable in Point of Nuclear Magnetic Resonance and Natural Bond Orbital Specifications. *Journal of Computational and Theoretical Nanoscience* **2014**, *11*, 1465-1471, https://doi.org/10.1166/jctn.2014.3519.
66. Monajjemi, M.; Ghiasi, R.; Ketabi, S.; Passdar, H.; Mollaamin, F. A Theoretical Study of Metal-Stabilised Rare Tautomers Stability: N4 Metalated Cytosine (M=Be2+, Mg2+, Ca2+, Sr2+ and Ba2+) in Gas Phase and Different. *Journal of Chemical Research* **2004**, *1*, 11-18, https://doi.org/10.3184/030823404323000648.
67. Monajjemi, M.; Baei, M.T.; Mollaamin, F. Quantum mechanic study of hydrogen chemisorptions on nanocluster vanadium surface. *Russian Journal of Inorganic Chemistry* **2008**, *53*, 1430-1437, https://doi.org/10.1134/S0036023608090143.
68. Mollaamin, F.; Baei, M.T.; Monajjemi, M.; Zhiani, R.; Honarparvar, B. A DFT study of hydrogen chemisorption on V (100) surfaces. *Russian Journal of Physical Chemistry A, Focus on Chemistry* **2008**, *82*, 2354-2361, https://doi.org/10.1134/S0036024408130323.
69. Monajjemi, M.; Honarparvar, B.; Nasseri, S.M.; Khaleghian, M. NQR and NMR study of hydrogen bonding interactions in anhydrous and monohydrated guanine cluster model: A computational study. *Journal of Structural Chemistry* **2009**, *50*, 67-77, https://doi.org/10.1007/s10947-009-0009-z.
70. Monajjemi, M.; Aghaie, H.; Naderi, F. Thermodynamic study of interaction of TSPP, CoTsPc, and FeTsPc with calf thymus DNA. *Biochemistry (Moscow)* **2007**, *72*, 652-657.
71. Monajjemi, M.; Heshmat, M.; Aghaei, H.; Ahmadi, R.; Zare, K. Solvent effect on 14N NMR shielding of glycine, serine, leucine, and threonine: Comparison between chemical shifts and energy versus dielectric constant. *Bulletin of the Chemical Society of Ethiopia* **2007**, *21*, 111-116, https://doi.org/10.4314/bcse.v21i1.61387.
72. Monajjemi, M.; Rajaeian, E.; Mollaamin, F.; Naderi, F.; Saki, S. Investigation of NMR shielding tensors in 1,3 dipolar cycloadditions: solvents dielectric effect. *Physics and Chemistry of Liquids* **2008**, *46*, 299-306, https://doi.org/10.1080/00319100601124369.
73. Mollaamin, F.; Varmaghani, Z.; Monajjemi, M. Dielectric effect on thermodynamic properties in vinblastine by DFT/Onsager modelling. *Physics and Chemistry of Liquids* **2011**, *49*, 318-336, https://doi.org/10.1080/00319100903456121.
74. Monajjemi, M.; Honaparvar, B.; Khalili Hadad, B.; Ilkhani, A.; Mollaamin, F. Thermo-Chemical Investigation and NBO Analysis of Some anxileotic as Nano- Drugs. *African journal of pharmacy and pharmacology* **2010**, *4*, 521-529.
75. Monajjemi, M.; Khaleghian, M.; Mollaamin, F. Theoretical study of the intermolecular potential energy and second virial coefficient in the mixtures of CH4 and Kr gases: a comparison with experimental data. *Molecular Simulation* **2010**, *36*, 865-870, https://doi.org/10.1080/08927022.2010.489557.
76. Monajjemi, M.; Khosravi, M.; Honarparvar, B.; Mollaamin, F. Substituent and solvent effects on the structural bioactivity and anticancer characteristic of catechin as a bioactive constituent of green tea. *International Journal of Quantum Chemistry* **2011**, *111*, 2771-2777, https://doi.org/10.1002/qua.22612.

77. Tahan, A.; Monajjemi, M. Solvent dielectric effect and side chain mutation on the structural stability of Burkholderia cepacia lipase active site: a quantum mechanical/molecular mechanics study. *Acta Biotheor* **2011**, *59*, 291-312, https://doi.org/10.1007/s10441-011-9137-x.
78. Monajjemi, M.; Khaleghian, M. EPR Study of Electronic Structure of [CoF6]3-and B18N18 Nano Ring Field Effects on Octahedral Complex. *Journal of Cluster Science* **2011**, *22*, 673-692, https://doi.org/10.1007/s10876-011-0414-2.
79. Monajjemi, M.; Mollaamin, F. Molecular Modeling Study of Drug-DNA Combined to Single Walled Carbon Nanotube. *Journal of Cluster Science* **2012**, *23*, 259-272, https://doi.org/10.1007/s10876-011-0426-y.
80. Mollaamin, F.; Monajjemi, M. Fractal Dimension on Carbon Nanotube-Polymer Composite Materials Using Percolation Theory. *Journal of Computational and Theoretical Nanoscience* **2012**, *9*, 597-601, https://doi.org/10.1166/jctn.2012.2067.
81. Mahdavian, L.; Monajjemi, M. Alcohol sensors based on SWNT as chemical sensors: Monte Carlo and Langevin dynamics simulation. *Microelectronics Journal* **2010**, *41*, 142-149, https://doi.org/10.1016/j.mejo.2010.01.011.
82. Monajjemi, M.; Falahati, M.; Mollaamin, F. Computational investigation on alcohol nanosensors in combination with carbon nanotube: a Monte Carlo and ab initio simulation. *Ionics* **2013**, *19*, 155-164, https://doi.org/10.1007/s11581-012-0708-x.
83. Tahan, A.; Mollaamin, F.; Monajjemi, M. Thermochemistry and NBO analysis of peptide bond: Investigation of basis sets and binding energy. *Russian Journal of Physical Chemistry A* **2009**, *83*, 587-597, https://doi.org/10.1134/S003602440904013X
84. Kapur, M.; Ganguly, A.; Nagy, G.; Adamson, S.I.; Chuang, J.H.; Frankel, W.N.; Ackerman, S.L. Expression of the Neuronal tRNA n-Tr20 Regulates Synaptic Transmission and Seizure Susceptibility. *Neuron* **2020**, *108*, 193–208, https://doi.org/10.1016/j.neuron.2020.07.023.
85. Qin, C.; Xu, P.-P.; Zhang, X.; Zhang, C.; Liu, C.-B.; Yang, D.-G.; Gao, F.; Yang, M.-L.; Du, L.-J.; Li, J.-J. Pathological significance of tRNA-derived small RNAs in neurological disorders. *Neural Regen. Res.* **2020**, *15*, 212–221, https://doi.org/10.4103/1673-5374.265560.
86. Vuokila, N.; Das Gupta, S.; Huusko, R.; Tohka, J.; Puhakka, N.; Pitkänen, A. Elevated Acute Plasma miR-124-3p Level Relates to Evolution of Larger Cortical Lesion Area after Traumatic Brain Injury. *Neuroscience* **2020**, *433*, 21–35, https://doi.org/10.1016/j.neuroscience.2020.02.045.
87. Wu, J.; He, J.; Tian, X.; Luo, Y.; Zhong, J.; Zhang, H.; Li, H.; Cen, B.; Jiang, T.; Sun, X. microRNA-9-5p alleviates blood-brain barrier damage and neuroinflammation after traumatic brain injury. *J. Neurochem.* **2020**, *153*, 710–726, https://doi.org/10.1111/jnc.14963.
88. Korotkov, A.; Puhakka, N.; Gupta, S.D.; Vuokila, N.; Broekaart, D.W.M.; Anink, J.J.; Heiskanen, M.; Karttunen, J.; van Scheppingen, J.; Huitinga, I.; Mills, J.D.; van Vliet, E.A.; Pitkänen, A.; Aronica, E. Increased expression of miR142 and miR155 in glial and immune cells after traumatic brain injury may contribute to neuroinflammation via astrocyte activation. *Brain Pathol.* **2020**, *30*, 897–912, https://doi.org/10.1111/bpa.12865.
89. Zhang, L.; Liu, C.; Huang, C.; Xu, X.; Teng, J. miR-155 Knockdown Protects against Cerebral Ischemia and Reperfusion Injury by Targeting MafB. *Biomed Res. Int.* **2020**, *2020*, https://doi.org/10.1155/2020/6458204.
90. Avcilar-Kucukgoze, I.; Kashina, A. Hijacking tRNAs From Translation: Regulatory Functions of tRNAs in Mammalian Cell Physiology. *Front. Mol. Biosci.* **2020**, *7*, https://doi.org/10.3389/fmolb.2020.610617.
91. Xie, Y.; Yao, L.; Yu, X.; Ruan, Y.; Li, Z.; Guo, J. Action mechanisms and research methods of tRNA-derived small RNAs. *Signal Transduct. Target. Ther.* **2020**, *5*, https://doi.org/10.1038/s41392-020-00217-4.
92. Cool, C.D.; Kuebler, W.M.; Bogaard, H.J.; Spiekerkoetter, E.; Nicolls, M.R.; Voelkel, N.F. The Hallmarks of Severe Pulmonary Arterial Hypertension: The Cancer Hypothesis - Ten years later. *Am. J. Physiol. Cell. Mol. Physiol.* **2020**, https://doi.org/10.1152/ajplung.00476.2019.
93. Sommer, N.; Ghofrani, A.; Pak, O.; Bonnet, S.; Provencher, S.; Sitbon, O.; Rosenkranz, S.; Hoeper, M.M.; Kiely, D.G. Current and future treatments of pulmonary arterial hypertension. *Br. J. Pharmacol.* **2020**, https://doi.org/10.1111/bph.15016.
94. Sindi, H.A.; Russomanno, G.; Satta, S.; Abdul-Salam, V.B.; Jo, K.B.; Qazi-Chaudhry, B.; Ainscough, A.J.; Szulcek, R.; Jan Bogaard, H.; Morgan, C.C.; Pullamsetti, S.S.; Alzaydi, M.M.; Rhodes, C.J.; Piva, R.; Eichstaedt, C.A.; Grünig, E.; Wilkins, M.R.; Wojciak-Stothard, B. Therapeutic potential of KLF2-induced exosomal microRNAs in pulmonary hypertension. *Nature Communications* **2020**, *11*, 1–17, https://doi.org/10.1038/s41467-020-14966-x.
95. Agostini, M.; Ganini, C.; Candi, E.; Melino, G. The role of noncoding RNAs in epithelial cancer. *Cell Death Discov.* **2020**, *6*, 1–12, https://doi.org/10.1038/s41420-020-0247-6.
96. Monajjemi, M.; Mahdavian, L.; Mollaamin, F.; Khaleghian, M. Interaction of Na, Mg, Al, Si with carbon nanotube (CNT): NMR and IR study. *Russ. J. Inorg. Chem* **2009**, *54*, 1465-1473. https://doi.org/10.1134/S0036023609090216
97. Bonnet, S.; Boucherat, O.; Paulin, R.; Wu, D.; Hindmarch, C.C.T.; Archer, S.L.; Song, R.; Moore, J.B.; Provencher, S.; Zhang, L.; Uchida, S. Clinical value of non-coding RNAs in cardiovascular, pulmonary, and muscle diseases. *Am. J. Physiol. Physiol.* **2020**, *318*, C1–C28, https://doi.org /10.1152/ ajpcell.00078.2019.

98. Ghalandari, B.; Monajjemi, M.; Mollaamin, F. Theoretical Investigation of Carbon Nanotube Binding to DNA in View of Drug Delivery. *J.Comput.Theor.Nanosci* **2011**, *8*, 1212-1219, https://doi.org/10.1166/jctn.2011.1801.
99. Magee, R.; Rigoutsos, I. On the expanding roles of tRNA fragments in modulating cell behavior. *Nucleic Acids Res.* **2020**, *48*, 9433–9448, https://doi.org/10.1093/nar/gkaa657.
100. Green, J.; Ansari, M.Y.; Ball, H.; Haqqi, T.M. tRNA-derived fragments (tRFs) regulate posttranscriptional gene expression via AGO-dependent mechanism in IL-1β stimulated chondrocytes. *Osteoarthr. Cartil.* **2020**, *28*, 1102–1110, https://doi.org/10.1016/j.joca.2020.04.014.
101. Khaleghian, M.; Zahmatkesh, M.; Mollaamin, F.; Monajjemi, M. Investigation of Solvent Effects on Armchair Single-Walled Carbon Nanotubes: A QM/MD Study. *Fuller. Nanotub. Carbon Nanostructures.*,**2011,** *19*, 251-261, https://doi.org/10.1080/1536.
102. Vilardo, E.; Amman, F.; Toth, U.; Kotter, A.; Helm, M.; Rossmanith, W. Functional characterization of the human tRNA methyltransferases TRMT10A and TRMT10B. *Nucleic Acids Res.* **2020**, *48*, 6157–6169, https://doi.org/10.1093/nar/gkaa353.
103. Ontiveros, R.J.; Shen, H.; Stoute, J.; Yanas, A.; Cui, Y.; Zhang, Y.; Liu, K.F. Coordination of mRNA and tRNA methylations by TRMT10A. *Proc. Natl. Acad. Sci. USA* **2020**, *117*, 7782–7791, https://doi.org/10.1073/pnas.1913448117.
104. Kobiita, A.; Godbersen, S.; Araldi, E.; Ghoshdastider, U.; Schmid, M.W.; Spinas, G.; Moch, H.; Stoffel, M. The Diabetes Gene JAZF1 Is Essential for the Homeostatic Control of Ribosome Biogenesis and Function in Metabolic Stress. *Cell Rep.* **2020**, *32*, https://doi.org/10.1016/j.celrep.2020.107846.
105. Mollaamin, F.; Monajjemi, M. Harmonic Linear Combination and Normal Mode Analysis of Semiconductor Nanotubes Vibrations. *J. Comput. Theor. Nanosci* **2015**, *12*, 1030-1039. https://doi.org/10.1166/jctn.2015.3846.
106. Kaspar, D.; Hastreiter, S.; Irmler, M.; De Angelis, M.H.; Beckers, J. Nutrition and its role in epigenetic inheritance of obesity and diabetes across generations. *Mamm. Genome* **2020**, *31*, 119–133, https://doi.org/10.1007/s00335-020-09839-z.
107. Nätt, D.; Öst, A. Male reproductive health and intergenerational metabolic responses from a small RNA perspective. *J. Intern. Med.* **2020**, *288*, 305–320, https://doi.org/10.1111/joim.13096.
108. Eizirik, D.L.; Pasquali, L.; Cnop, M. Pancreatic β-cells in type 1 and type 2 diabetes mellitus: Different pathways to failure. *Nat.Rev. Endocrinol.* **2020**, *16*, 349–362, https://doi.org/10.1038/s41574-020-0355-7.
109. Lytrivi, M.; Castell, A.-L.; Poitout, V.; Cnop, M. Recent Insights Into Mechanisms of β-Cell Lipo- and Glucolipotoxicity in Type 2 Diabetes. *J. Mol. Biol.* **2020**, *432*, 1514–1534, https://doi.org/10.1016/j.jmb.2019.09.016.
110. Yu, M.; Lu, B.; Zhang, J.; Ding, J.; Liu, P.; Lu, Y. tRNA-derived RNA fragments in cancer: Current status and future perspectives. *J.Hematol. Oncol.* **2020**, *13*, 1–14, https://doi.org/10.1186/s13045-020-00955-6.
111. Ghosh, A.; Williams, L.D.; Pestov, D.G.; Shcherbik, N. Proteotoxic Stress Promotes Entrapment of Ribosomes and Misfolded Proteins in a Shared Cytosolic Compartment. *Nucleic Acids Res.* **2021**, *48*, 3888–3905, https://doi.org/10.1093/nar/gkaa068.
112. Beasley, A.B.; Acheampong, E.; Lin, W.; Gray, E.S. Multi-Marker Immunomagnetic Enrichment of Circulating Melanoma Cells. *Methods Mol. Biol.* **2021**, *2265*, 213–222, https://doi.org/10.1007/978-1-0716-1205-7_16.
113. Papanota, A.M.; Karousi, P.; Kontos, C.K.; Ntanasis-Stathopoulos, I.; Scorilas, A.; Terpos, E. Multiple Myeloma Bone Disease: Implication of MicroRNAs in Its Molecular Background. *Int. J. Mol. Sci.* **2021**, *22*, https://doi.org/10.3390/ijms22052375.
114. Zhou, Y.; Peng, H.; Cui, Q.; Zhou, Y. tRFTar: Prediction of tRF-target gene interactions via systemic re-analysis of Argonaute CLIP-seq datasets. *Methods* **2021**, *187*, 57–67, https://doi.org/10.1016/j.ymeth.2020.10.006.
115. Xu, C.; Liang, T.; Zhang, F.; Liu, J.; Fu, Y. tRNA-derived fragments as novel potential biomarkers for relapsed/refractory multiple myeloma. *BMC Bioinform.* **2021**, *22*, https://doi.org/10.1186/s12859-021-04167-8.
116. Katsaraki, K.; Adamopoulos, P.G.; Papageorgiou, S.G.; Pappa, V.; Scorilas, A.; Kontos, C.K. A 3' tRNA-derived fragment produced by tRNA(LeuAAG) and tRNA(LeuTAG) is associated with poor prognosis in B-cell chronic lymphocytic leukemia, independently of classical prognostic factors. *Eur. J. Haematol.* **2021**, *106*, 821–830, https://doi.org/10.1111/ejh.13613.
117. Xu, C.; Fu, Y. Expression Profiles of tRNA-Derived Fragments and Their Potential Roles in Multiple Myeloma. *OncoTargets Ther.***2021**, *14*, 2805–2814, https://doi.org/10.2147/ott.s302594.
118. Rojek, A.E.; Katanski, C.D.; Stefka, A.; Derman, B.A.; Jakubowiak, A.; Pan, T. Abstract 2394: tRNA expression and tRFs in multiple myeloma: Progression from monoclonal gammopathies to relapsed/refractory disease. *Cancer Res.* **2021**, *81*, https://doi.org/10.1158/1538-7445.AM2021-2394.
119. Papanota, A.M.; Tsiakanikas, P.; Kontos, C.K.; Malandrakis, P.; Liacos, C.I.; Ntanasis-Stathopoulos, I.; Kanellias, N.; Gavriatopoulou, M.; Kastritis, E.; Avgeris, M.; Dimopoulos, M.A.; Scorilas, A.; Terpos, E. A Molecular Signature of Circulating MicroRNA Can Predict Osteolytic Bone Disease in Multiple Myeloma. *Cancers (Basel)* **2021**, *13*, https://doi.org/10.3390/cancers13153877.

120. Papadimitriou, M.A.; Papanota, A.M.; Adamopoulos, P.G.; Pilala, K.M.; Liacos, C.I.; Malandrakis, P.; Mavrianou-Koutsoukou, N.; Patseas, D.; Eleutherakis-Papaiakovou, E.; Gavriatopoulou, M.; Kastritis, E.; Avgeris, M.; Dimopoulos, M.A.; Terpos, E.; Scorilas, A. miRNA-seq and clinical evaluation in multiple myeloma: miR-181a overexpression predicts short-term disease progression and poor post-treatment outcome. *British journal of cancer* **2022**, *126*, 79-90, https://doi.org/10.1038/s41416-021-01602-8.
121. Artemaki, P.I.; Letsos, P.A.; Zoupa, I.C.; Katsaraki, K.; Karousi, P.; Papageorgiou, S.G.; Pappa, V.; Scorilas, A.; Kontos, C.K. The Multifaceted Role and Utility of MicroRNAs in Indolent B-Cell Non-Hodgkin Lymphomas. *Biomedicines* **2021**, *9*, https://doi.org/10.3390/biomedicines9040333.
122. Krishna, S.; Raghavan, S.; DasGupta, R.; Palakodeti, D. tRNA-derived fragments (tRFs): establishing their turf in posttranscriptional gene regulation. *Cellular and Molecular Life Sciences* **2021**, *78*, 2607-2619, https://doi.org/10.1007/s00018-020-03720-7.
123. Sun, J.; Evans, P.N.; Gagen, E.J.; Woodcroft, B.J.; Hedlund, B.P.; Woyke, T.; Hugenholtz, P.; Rinke, C. Recoding of stop codons expands the metabolic potential of two novel Asgardarchaeota lineages. *ISME Communications* **2021**, *1*, https://doi.org/10.1038/s43705-021-00032-0.
124. Del Toro, N.; Lessard, F.; Bouchard, J.; Mobasheri, N.; Guillon, J.; Igelmann, S.; Tardif, S.; Buffard, T.; Bourdeau, V.; Brakier-Gingras, L. Cellular senescence limits translational readthrough. *Biology open* **2021**, *10*, https://doi.org/10.1242/bio.058688.
125. Valentini, G.D.T.; Valentini, G.P.T. Archaeal tRNA-Splicing Endonuclease as an Effector for RNA, Recombination and Novel Trans-Splicing Pathways in Eukaryotes. *J. Fungi* **2021**, *7*, https://doi.org/10.3390/jof7121069.